Eur. Phys. J. D **22**, 373–383 (2003)
DOI: 10.1140/epjd/e2003-00036-6

THE EUROPEAN PHYSICAL JOURNAL D

Coherence properties of two trapped particles

S. Franke-Arnold[1,a], S.M. Barnett[1], G. Huyet[2], and C. Sailliot[2]

[1] Department of Physics, University of Strathclyde, Glasgow G4 0NG, Scotland, UK
[2] Physics Department, National University of Ireland, University College, Cork, Ireland, UK

Received 19 September 2002
Published online 4 February 2003 –

Abstract. We analyse the coherence properties of two particles trapped in a one-dimensional harmonic potential. This simple model allows us to derive analytic expressions for the first and second order coherence functions. We investigate their properties depending on the particle nature and the temperature of the quantum gas. We find that at zero temperature non-interacting bosons and fermions show very different correlations, while they coincide for higher temperatures. We observe atom bunching for bosons and atom anti-bunching for fermions. When the effect of *s*-wave scattering between bosons is taken into account, we find that the range of coherence is enhanced or reduced for repulsive or attractive potentials, respectively. Strongly repelling bosons become in some way more "fermion-like" and show anti-bunching. Their first order coherence function, however, differs from that for fermions.

PACS. 05.30.-d Quantum statistical mechanics – 03.75.-b Matter waves – 42.50.Lc Quantum fluctuations, quantum noise, and quantum jumps

1 Introduction

The experimental realisation of Bose-Einstein condensation [1] has led to the elaboration of a theory of the coherence of matter waves [2] in analogy with the coherence theory of light [3,4]. In fact, the strong coherence of cold bosons is one of the most fascinating features of a quantum gas and was observed in the form of interferences and measurements of first and higher order coherence functions [5,6]. With increasing temperature the coherence diminishes and the atomic cloud behaves increasingly as an ensemble of particles rather than a macroscopic quantum object [7–9].

The coherence properties of a quantum gas can be calculated from the single and two particle density matrices and depend on the nature of the particles, their interactions and the temperature. In most cases, there is no analytic expression for the required density matrices and the coherence properties are evaluated numerically within the mean field theory. Although this approach yields good agreement with experiments, it can be hard to follow the underlying physics through the process. In this paper we present a different approach: by considering exactly two trapped particles in a one-dimensional harmonic potential we are able to calculate the two-particle states explicitly [10]. This allows us to find analytic solutions for the coherence functions and in particular for the effect of interaction on the coherence. We would like to mention related work by Markus Cirone and coworkers [11] who, using a similar approach, were able to investigate the influence of interaction on the formation of Bose Einstein condensation for two particles.

To first order, the interaction is described by *s*-wave scattering and can be modelled by a Dirac delta function potential. As *s*-wave scattering is not allowed for fermions we treat them as interaction free. It is worthwhile noticing that, in the limit of infinite interaction strength, the Dirac delta potential describes a Tonks gas [12], *i.e.* one-dimensional hard-core particles of infinitely small size. Tonks gasses at zero temperature have exact many body energy eigensolutions, so that their coherence properties can be calculated analytically. Unlike our model, they can contain an arbitrary number of particles, however, an extension to higher temperatures is more problematic.

Many features of quantum gas coherence are already manifest in the physics of our simple two-particle model: we observe that non-interacting bosons show coherence in wider regions than fermions. The degree of second order coherence displays bunching for bosons while anti-bunching is observed for fermions. For interacting bosons we find that a short range repulsive force enhances the range of coherence and decreases bunching effects, while an attractive force reduces the range of coherence and increases bunching effects. Indeed, bosons with a repulsive potential can present properties that are usually associated with fermions, and we compare the coherence properties of two strongly repelling bosons with those of two non-interacting fermions. The effect of interaction on the behaviour at a particle beam splitter has previously been studied in [13]. In this case the interaction between bosons

[a] e-mail: sonja@phys.strath.ac.uk

was shown to render the output statistics more fermion-like, irrespective of the sign of the interaction potential.

2 Wave functions for two trapped particles

Quantum gasses are usually described within the second quantisation formalism in the grand canonical ensemble. In this paper, we deal with coherence properties of exactly two particles and thus work in the canonical ensemble. This allows us to express the coherence properties of the two trapped atoms as a function of their two-particle wave function which we will derive in this section. We restrict ourselves to a one-dimensional geometry in which the interaction between the particles can be modelled by a delta function [10]. Such one-dimensional harmonic trapping potentials are realised in waveguide experiments as reported in [14].

The Hamiltonian for two particles of mass m trapped in a harmonic potential of frequency ω is

$$H = \frac{x_1^2}{2} + \frac{p_1^2}{2} + \frac{x_2^2}{2} + \frac{x_2^2}{2} + U(|x_1 - x_2|), \qquad (1)$$

where $x_{1,2}$ designate the positions of the two particles, $p_{1,2}$ their momenta, and U the interaction potential between the particles. We are using harmonic oscillator units with positions given in units of $\sqrt{\hbar/m\omega}$, momenta in units of $\sqrt{\hbar m\omega}$ and energies in units of $\hbar\omega$. Note that for two identical particles the potential has to be an even function of their relative positions. This Hamiltonian can be separated into a Hamiltonian for the motion of the centre of mass, H_c, and a Hamiltonian for the relative motion, H_r, by introducing the new operators: $x_\mathrm{c} = (x_1 + x_2)/\sqrt{2}$, $p_\mathrm{c} = (p_1 + p_2)/\sqrt{2}$, $x_\mathrm{r} = (x_1 - x_2)/\sqrt{2}$ and $p_\mathrm{r} = (p_1 - p_2)/\sqrt{2}$. The Hamiltonian can then be written as $H = H_\mathrm{c} + H_\mathrm{r}$, with

$$H_\mathrm{c} = \frac{1}{2}(p_\mathrm{c}^2 + x_\mathrm{c}^2), \qquad (2)$$

$$H_\mathrm{r} = \frac{1}{2}\left(p_\mathrm{r}^2 + x_\mathrm{r}^2\right) + U\left(\sqrt{2}|x_\mathrm{r}|\right). \qquad (3)$$

The motion of the centre of mass is governed by a harmonic oscillator Hamiltonian and the normal modes are the well-known number states $|n\rangle$ with dimensionless energies $E_n = n$, for $n = 0, 1, 2, ...$, ignoring the zero-point energy. The centre-of-mass modes in position representation are

$$u_n(x_\mathrm{c}) = \langle x_\mathrm{c}|n\rangle = \frac{1}{\pi^{1/4}2^{n/2}n!^{1/2}}\mathrm{H}_n(x_\mathrm{c})\mathrm{e}^{-x_\mathrm{c}^2/2}, \qquad (4)$$

where H_n denotes the nth Hermite polynomial. The eigenstates $|\nu\rangle$ of the relative motion and their energies $E_\nu = \nu$ depend on the potential U, where $\{\nu\}$ is a set of real numbers for a given potential. As the potential is an even function of x_r, the Hamiltonian H_r commutes with the parity operator. We denote the normalised eigenmodes of H_r by $w_\nu(x_\mathrm{r})$. Bosons require symmetric wavefunctions in x_r and fermions antisymmetric ones. Consequently, only the even functions in x_r are bosonic eigenmodes, the odd functions are fermionic eigenmodes, and both are eigenmodes for distinguishable particles. It is convenient to introduce the general mode function

$$v_\nu(x_\mathrm{r}) = \langle x_\mathrm{r}|\nu\rangle = \frac{w_\nu(x_\mathrm{r}) + b w_\nu(-x_\mathrm{r})}{1 + b^2}, \qquad (5)$$

in order to take into account the symmetry properties of the two-particle wavefunction, where $b = +1$ for bosons, 0 for distinguishable particles and -1 for fermions. The eigenstates of the two-particle system can then be described by $|n, \nu\rangle$ which obey $H|n, \nu\rangle = (n + \nu)|n, \nu\rangle$.

2.1 Non-interacting particles

For non-interacting particles, *i.e.* $U(x) = 0$, the relative motion as well as the centre of mass motion are governed by a harmonic oscillator Hamiltonian, with eigenmodes given by the number states (4). However, only number states that are compatible with the particle-nature dependent symmetry are allowed. This means that the relative motion of bosons/fermions is described by the even/odd number states, respectively, whereas distinguishable particles can be in any number state. According to equation (5) the symmetrised modes for the relative motion can formally be written as

$$v_\nu(x_\mathrm{r}) = \frac{u_\nu(x_\mathrm{r}) + b u_\nu(-x_\mathrm{r})}{1 + b^2}, \qquad (6)$$

where $\nu = 0, 1, 2, ...$

2.2 Interacting particles

The interaction between particles can be described to first order by s-wave scattering which does not occur for fermions. For this reason, we will concentrate on the effect of interaction on the coherence of bosons and distinguishable particles. For cold particles, s-wave scattering can be modelled by a point-like potential of zero range, as the finer details of the interaction potential become unimportant compared to their large de-Broglie wavelength. In one dimension, a zero-range potential can be represented by a Dirac delta function [1,10]:

$$U(|x_1 - x_2|) = a\delta(x_1 - x_2), \qquad (7)$$

where a is the interaction strength a. The resulting Hamiltonian for the relative motion (3) is

$$H_\mathrm{r} = \frac{p_\mathrm{r}^2}{2} + \frac{x_\mathrm{r}^2}{2} + a\delta(\sqrt{2}x_\mathrm{r}). \qquad (8)$$

The eigenmodes $w_\nu(x_\mathrm{r})$ can therefore be determined as the solutions of the Schrödinger equation

$$-\frac{1}{2}\frac{\partial^2 w_\nu(x_\mathrm{r})}{\partial x_\mathrm{r}^2} + \frac{1}{2}x_\mathrm{r}^2 w_\nu(x_\mathrm{r}) + \frac{a}{\sqrt{2}}\delta(x_\mathrm{r})\, w_\nu(x_\mathrm{r}) = \nu w_\nu(x_\mathrm{r}). \qquad (9)$$

This equation is solved by combinations of parabolic cylinder functions $D_\nu(\sqrt{2}x_\mathrm{r})$ [15]. The boundary conditions at $x \to \pm\infty$ as well as the behaviour at $x = 0$ determine the choice of functions and the value of ν for a given interaction strength a. We note that for $a = 0$ the Schrödinger equation reduces to the harmonic oscillator equation. In this case ν is integer, and $D_\nu(\sqrt{2}x_\mathrm{r})$ are proportional to the number state wavefunctions (4). We note that equation (9) is identical to the harmonic oscillator equation at $x_\mathrm{r} \neq 0$. This means that the odd eigenmodes w_{2m+1}, which are zero at $x_\mathrm{r} = 0$, will not be altered by the interaction potential and are still given by the odd number states. The even eigenmodes are given by

$$w_\nu(x_\mathrm{r}) = \frac{D_\nu\left(\sqrt{2}|x_\mathrm{r}|\right)}{\sqrt{2\int_0^{+\infty} D_\nu^2\left(\sqrt{2}x_\mathrm{r}\right)\mathrm{d}x_\mathrm{r}}}, \tag{10}$$

which are normalised so that $\int_{-\infty}^{+\infty}\mathrm{d}x\, v_\nu^2(x) = 1$. The eigenfunctions of interacting bosons are therefore given by the parabolic cylinder functions, whereas the eigenfunctions of interacting distinguishable particles alternate between the parabolic cylinder functions and the odd number states. The value of ν can be determined by integrating (9) over x_r between $-\epsilon$ and $+\epsilon$ and taking the limit $\epsilon \to 0$. This leads to

$$-w'_\nu(0^+) + \frac{a}{\sqrt{2}} w_\nu(0) = 0. \tag{11}$$

Here we have used the fact that $w'_\nu(0^-) = -w'_\nu(0^+)$, as the derivative of the even function v_ν is odd. The value of the parabolic cylinder function and its derivative at the origin are [15] $D_\nu(0) = 2^{\nu/2}\sqrt{\pi}/\Gamma\left(1/2 - \nu/2\right), D'_\nu(0+) = -2^{\nu/2+1/2}\sqrt{\pi}/\Gamma\left(-\nu/2\right)$. By inserting these values into equation (11), keeping in mind that $v'_\nu \sim \sqrt{2}D'_\nu$, we find that the set of possible energies ν is related to the interaction strength a by

$$2^{3/2}\frac{\Gamma\left(\frac{1}{2} - \frac{\nu}{2}\right)}{\Gamma\left(-\frac{\nu}{2}\right)} + a = 0. \tag{12}$$

The energy levels as a function of the interaction strength are shown in Figure 5a. For an attractive potential, *i.e.* $a < 0$, the energy is reduced compared to the corresponding harmonic oscillator level, and for a repulsive potential, *i.e.* $a > 0$, increased. The even number states have extrema at $x_\mathrm{r} = 0$, which are "dented" by an attractive or repulsive potential as shown in Figures 5b–5g. In fact, an infinitely strong repulsive interaction generates a node at $x_\mathrm{r} = 0$, whereas for $x_\mathrm{r} \neq 0$ the eigenmodes still have to be solutions of the harmonic oscillator. The squared modulus therefore becomes identical to that of the next higher (odd) number state. Similarly, the squared modulus of the wavefunction in an infinitely strong attractive potential becomes identical to that of the next lower (odd) number state, with the exception of the ground state. Thus the energies of the higher order states increases from $\hbar\omega(2n-1)$ to $\hbar\omega(2n+1)$ when a increases from $-\infty$ to $+\infty$, while the energy of the ground state increases from minus infinity to unity when a increases from $-\infty$ to $+\infty$. The eigenenergies of bosons subject to an infinitely strong repulsive potential are the same as the eigenenergies of non-interacting fermions. This is reminiscent of the energy structure of Tonks gasses: the many body energy eigensolutions of Tonks gasses are found using the mapping theorem [12] to a gas of spinless fermions. As a result, Tonks gasses have the same density but different coherence properties as fermions.

3 Coherence properties

Generally, the coherence properties of matter waves can be described in terms of the operators $\hat{\psi}(x)$ and $\hat{\psi}^\dagger(x)$ [2] which annihilate and create, respectively, a particle at the position x. These operators satisfy the commutation relation $[\hat{\psi}(x), \hat{\psi}^\dagger(y)]_\mathrm{B} = \delta(x-y)$ for bosons and the anti-commutation relation $\{\hat{\psi}(x), \hat{\psi}^\dagger(y)\}_\mathrm{F} = \delta(x-y)$ for fermions. With the subscripts B and F we denote bosons and fermions, respectively. We normally assume, that the two particles in the trap are indistinguishable. However, if each particle is in a different internal quantum state they become distinguishable, and are each associated with an individual generation and annihilation operator $\hat{\psi}_1^\dagger(x), \hat{\psi}_2^\dagger(x), \hat{\psi}_1(x), \hat{\psi}_2(x)$. In this case, operators belonging to different particles will commute if they are bosons and anticommute if they are fermions $[\hat{\psi}_i(x), \hat{\psi}_j^\dagger(y)]_\mathrm{B} = \delta_{ij}\delta(x-y)$ and $\{\hat{\psi}_i(x), \hat{\psi}_j^\dagger(y)\}_\mathrm{F} = \delta_{ij}\delta(x-y)$.

The coherence properties of the atoms are apparent in interference experiments. These can display interference of amplitudes or of intensity. The quality of interference for amplitudes and intensities is measured by the first and second order coherence function, respectively. For indistinguishable particles, these are defined as

$$G^{(1)}_{\mathrm{B,F}}(x,y) = \left\langle \hat{\psi}^\dagger(x)\,\hat{\psi}(y)\right\rangle, \tag{13}$$

$$G^{(2)}_{\mathrm{B,F}}(x,y) = \left\langle \hat{\psi}^\dagger(x)\,\hat{\psi}^\dagger(y)\,\hat{\psi}(y)\,\hat{\psi}(x)\right\rangle. \tag{14}$$

For distinguishable particles, however, we need to consider the internal degree of freedom. We will assume that the detection process is not sensitive to the internal quantum number by which the particles may be distinguished. This is to make a comparison with bosons and fermions for which such a distinction is impossible, even in principle. We note, however, that as we could at least in principle identify the detected particle, there is no interference associated with $\langle\hat{\psi}_1^\dagger(x)\,\hat{\psi}_2(y)\rangle$ and similar terms. The coherence functions for distinguishable particles are therefore

$$G^{(1)}_\mathrm{D}(x,y) = \left\langle \hat{\psi}_1^\dagger(x)\,\hat{\psi}_1(y)\right\rangle + \left\langle \hat{\psi}_2^\dagger(x)\,\hat{\psi}_2(y)\right\rangle, \tag{15}$$

$$G^{(2)}_\mathrm{D}(x,y) = \left\langle \hat{\psi}_1^\dagger(x)\,\hat{\psi}_2^\dagger(y)\,\hat{\psi}_2(y)\,\hat{\psi}(x)_1\right\rangle + \left\langle \hat{\psi}_2^\dagger(x)\,\hat{\psi}_1^\dagger(y)\,\hat{\psi}_1(y)\,\hat{\psi}(x)_2\right\rangle. \tag{16}$$

In order to remove the effects of density variations, it is useful to define normalised versions of the coherence

functions, the degrees of first and second order coherence:

$$g^{(1)}(x,y) = \frac{G^{(1)}(x,y)}{\sqrt{G^{(1)}(x,x)\,G^{(1)}(y,y)}}, \quad (17)$$

$$g^{(2)}(x,y) = \frac{G^{(2)}(x,y)}{G^{(1)}(x,x)\,G^{(1)}(y,y)}\,. \quad (18)$$

The modulus of the degree of first order coherence measures the correlation between the positions x and y. As we are dealing with exactly two particles, the degree of second order coherence is proportional the probability that one particle is found at x and the other at y. It is evident, that $g^{(2)}(x,y)$ depends crucially on the spin statistics of the wavefunction. In the following we will write the first and second order coherence functions in terms of the eigenmodes u_n and v_ν and evaluate the averages in the basis of the two-particle states $|n,\nu\rangle$. We can construct the two-particle state $|n,\nu\rangle$ by applying the generation operators $\hat{\psi}^\dagger(x_1)$ and $\hat{\psi}^\dagger(x_2)$ onto the vacuum or no-particle state $|\mathrm{vac}\rangle$, and integrating over the centre of mass mode function $u_n((x_1+x_2)/\sqrt{2})$ and the relative mode function $w_\nu((x_1-x_2)/\sqrt{2})$. The normalised two-particle state can then be written as

$$|n,\nu\rangle_{\mathrm{B,F}} = \frac{1}{\sqrt{2}}\int \mathrm{d}x_1\mathrm{d}x_2\, u_n\left(\frac{x_1+x_2}{\sqrt{2}}\right) w_\nu\left(\frac{x_1-x_2}{\sqrt{2}}\right) \times \hat{\psi}^\dagger(x_1)\hat{\psi}^\dagger(x_2)|\mathrm{vac}\rangle \quad (19)$$

$$|n,\nu\rangle_{\mathrm{D}} = \int \mathrm{d}x_1\mathrm{d}x_2\, u_n\left(\frac{x_1+x_2}{\sqrt{2}}\right) w_\nu\left(\frac{x_1-x_2}{\sqrt{2}}\right) \times \hat{\psi}_1^\dagger(x_1)\hat{\psi}_2^\dagger(x_2)|\mathrm{vac}\rangle\,. \quad (20)$$

For bosons $\hat{\psi}^\dagger(x_1)\hat{\psi}^\dagger(x_2) = \hat{\psi}^\dagger(x_2)\hat{\psi}^\dagger(x_1)$ so that the integral vanishes for odd functions w_ν, whereas for fermions $\hat{\psi}^\dagger(x_1)\hat{\psi}^\dagger(x_2) = -\hat{\psi}^\dagger(x_2)\hat{\psi}^\dagger(x_1)$ so that the integral vanishes for even functions w_ν. For distinguishable particles both even and odd functions w_ν are possible. This means that the states with allowed symmetries are selected automatically. In the remaining sections we will study the behaviour of thermal states. In this case the density matrix is diagonal in n and ν and we can write the density matrix as

$$\rho = \sum_{n,\nu} P_{n,\nu}|n,\nu\rangle\langle n,\nu|, \quad (21)$$

where $P_{n,\nu}$ is the probability that the state $|n,\nu\rangle$ is occupied. By expressing the expectation value in (13) *via* the density matrix we find

$$G^{(1)}(x,y) = \sum_{n,\nu} P_{n,\nu}\left\langle n,\nu\left|\hat{\psi}^\dagger(x)\,\hat{\psi}(y)\right|n,\nu\right\rangle. \quad (22)$$

We can now insert the two-particle state (19) for indistinguishable particles and use the corresponding commutation and anti-commutation relations. The first order coherence function can then be written as

$$G^{(1)}(x,y) = 2\int_{-\infty}^{+\infty}\mathrm{d}z\sum_{n,\nu} P_{n,\nu}u_n\left(\frac{z+y}{\sqrt{2}}\right)u_n^*\left(\frac{x+z}{\sqrt{2}}\right) \times v_\nu\left(\frac{z-y}{\sqrt{2}}\right)v_\nu^*\left(\frac{z-x}{\sqrt{2}}\right). \quad (23)$$

Note that by using equations (15, 19), the same expression can be found for distinguishable particles. The difference in evaluating $G^{(1)}$ for distinguishable or indistinguishable particles is inherent in the allowed states of the relative motion and in the values of the $P_{n,\nu}$.

Similarly we can derive the second order coherence function:

$$G^{(2)}(x,y) = \sum_{n,\nu} P_{n,\nu}\left\langle n,\nu\left|\hat{\psi}^\dagger(x)\,\hat{\psi}^\dagger(y)\,\hat{\psi}(y)\,\hat{\psi}(x)\right|n,\nu\right\rangle = 2\sum_{n,\nu} P_{n,\nu}\left|u_n\left(\frac{x+y}{\sqrt{2}}\right)v_\nu\left(\frac{x-y}{\sqrt{2}}\right)\right|^2. \quad (24)$$

It is worthwhile noticing that, for a pure state, the second order coherence function is proportional to the modulus squared of the two-particle wave function. From equations (23, 24), it is possible to calculate the coherence functions for any state of the two trapped interacting particles. In the following sections, we will use these expressions to analyse the coherence properties of two non-interacting thermal particles and then two interacting bosons or distinguishable particles.

4 Coherence properties of non-interacting particles

In this section we consider non-interacting particles. The centre of mass modes are given by the harmonic oscillator modes (4) and the modes of relative motion consist of the even, odd, or all harmonic oscillator modes for bosons, fermions, or distinguishable particles, respectively (6). We begin by evaluating the first order coherence function at zero and higher temperatures. At $T = 0$ we can evaluate $G^{(1)}$ directly from the second quantised formulae (13, 15). Bosons and distinguishable particles occupy the ground state of the harmonic oscillator so that the first order coherence function

$$G^{(1)}_{\mathrm{B,D}}(x,y) = 2u_0(x)u_0(y) = \frac{2}{\sqrt{\pi}}\exp\left(-\frac{x^2+y^2}{2}\right) \quad (25)$$

is a 2D Gaussian function as shown in Figures 1a and 1c. For fermions at zero temperature the single particle density matrix is in a mixture of the two lowest energy levels of the harmonic oscillator so that

$$G^{(1)}_{\mathrm{F}}(x,y) = u_0(x)u_0(y) + u_1(x)u_1(y) = \frac{1+2xy}{\sqrt{\pi}}\exp\left(-\frac{x^2+y^2}{2}\right) \quad (26)$$

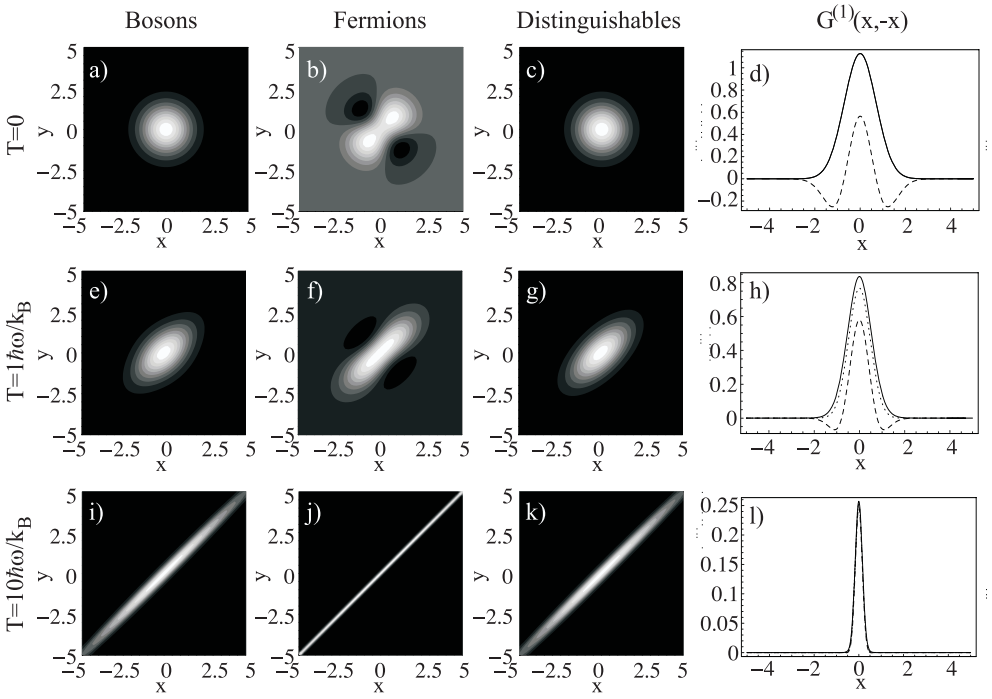

Fig. 1. Density plots of the first order coherence function $G^{(1)}(x,y)$ for (a) two bosons, (b) two fermions and (c) two distinguishable particles at the temperatures $T = 0$. Plot (d) shows $G^{(1)}(x,-x)$, *i.e.* the first order coherence function along the diagonal of the density plots. Here, bosons, fermions and distinguishable particles are displayed as solid, dashed and dotted lines, respectively. Similarly, plots (e) to (h) show the corresponding behaviour at $T = \hbar\omega/k_{\mathrm{B}}$ and plots (i) to (l) at $T = 10\hbar\omega/k_{\mathrm{B}}$. Note that the colours of each density plots are chosen such that black corresponds to the minimum value and white to the maximum value of the displayed function. Absolute values can be taken from the plots (d), (h) and (l).

as shown in Figure 1b. At zero temperature, the difference between bosons and fermions is most striking as fermions may occupy the mode u_1 but bosons or distinguishable particles do not. While the first order coherence functions of bosons is centered around $x = y = 0$, the one for fermions shows two peaks at $x = y = \pm 1/2$. This is associated with the "repelling force" between the Fermions. Unlike bosons and distinguishable particles, fermions show regions of negative values for $G^{(1)}_{\mathrm{F}}(x,y)$ with minima at $x = -y = \pm\sqrt{3/2}$, as can be seen in Figure 1d. These negative values indicate destructive interference which results when negative parts of one fermionic wavefunction overlap with positive parts of the other.

More generally, we consider non-interacting particles at finite temperature. At a temperature T the state $|n,\nu\rangle$ is occupied with the probability $P_{n,\nu} \propto \exp\left[-(n+\nu)\beta\hbar\omega\right]$, where $\beta = 1/k_{\mathrm{B}}T$ and k_{B} denotes the Boltzmann constant. By inserting (6) into the expression for $G^{(1)}(x,y)$ (23) one obtains

$$G^{(1)}(x,y) = \frac{\kappa\left(1+b^2\right)}{\sqrt{\tanh\left(\frac{\beta\hbar\omega}{2}\right)}} \exp\left(-\left(\frac{x+y}{2}\right)^2 \times \tanh\left(\frac{\beta\hbar\omega}{2}\right) - \left(\frac{x-y}{2}\right)^2 \coth\left(\frac{\beta\hbar\omega}{2}\right)\right) + 2\kappa b\sqrt{\tanh\beta\hbar\omega}\exp\left(-\left(\frac{x+y}{2}\right)^2 \times \tanh\left(\beta\hbar\omega\right) - \left(\frac{x-y}{2}\right)^2 \coth\left(\beta\hbar\omega\right)\right), \tag{27}$$

where

$$\kappa = \frac{1}{\sqrt{\pi}}\frac{2}{(1+b^2)\coth(\frac{\beta\hbar\omega}{2}) + 2b}\,. \tag{28}$$

Here we have used the identity

$$\sum_{n=0}^{+\infty} \mathrm{e}^{-\beta\hbar\omega n} u_n(x)\, u_n(y) = \frac{\exp\left(-\left(\frac{x+y}{2}\right)^2 \tanh\left(\frac{\beta\hbar\omega}{2}\right) - \left(\frac{x-y}{2}\right)^2 \coth\left(\frac{\beta\hbar\omega}{2}\right)\right)}{\sqrt{\pi}\sqrt{1-\mathrm{e}^{-2\beta\hbar\omega}}}. \tag{29}$$

In the limit of $T \to 0$, this equation coincides with the direct calculation from the second quantised formula presented above. While at low temperatures fermions and bosons show very different coherence properties, at high temperatures they behave similarly and, in fact, act like distinguishable particles. This is illustrated in Figure 1, where the temperature increases from $T = 0$ in the top row (a–d), *via* temperatures comparable to the trapping temperature $T = \hbar\omega/k_{\mathrm{B}}$ in the middle row (e–h) up to high temperatures of $T = 10\hbar\omega/k_{\mathrm{B}}$ in the bottom row (i–l). With rising temperature, the particles are in "increasingly mixed" states so that the Fermi-exclusion principle becomes less important. Mathematically this is manifest in the fact that the second term in equation (27) becomes negligible compared to the first term and hence the first order coherence functions for bosons, fermions and

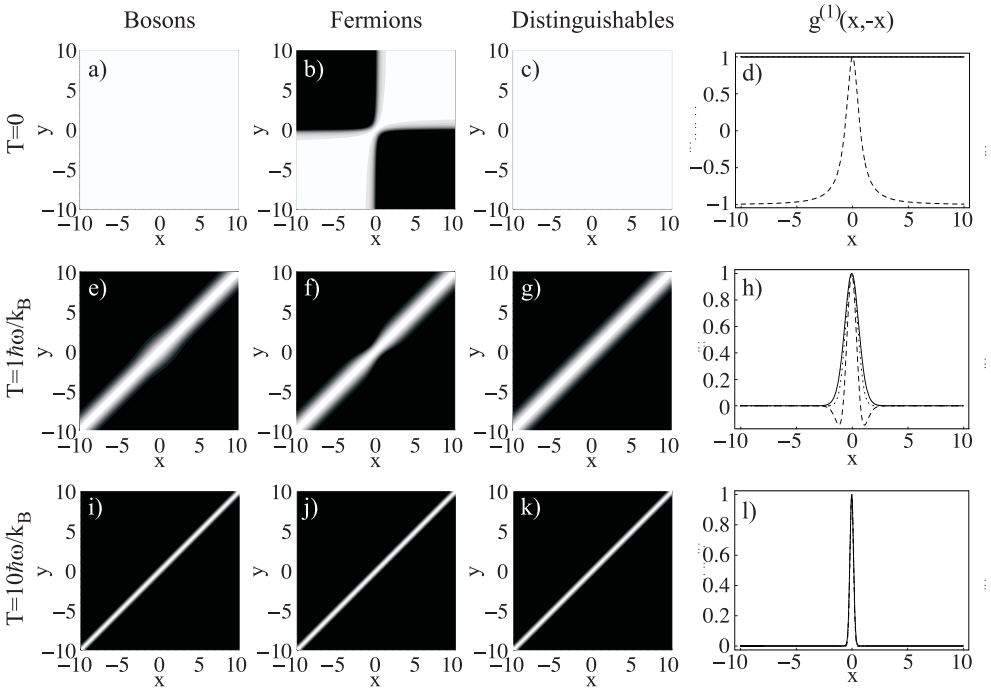

Fig. 2. Density plots of the degree of first order coherence $g^{(1)}(x, y)$ for two bosons, fermions and distinguishable particles at the temperatures $T = 0$, $T = \hbar\omega/k_{\mathrm{B}}$ and $T = 10\hbar\omega/k_{\mathrm{B}}$, displayed as in Figure 1.

distinguishable particles coincide:

$$G^{(1)}_{\mathrm{B,F,D}}(x, y) \simeq \frac{2\beta\hbar\omega}{\sqrt{\pi \tanh\left(\frac{\beta\hbar\omega}{2}\right)}} \exp\left(-\left(\frac{x+y}{2}\right)^2 \times \tanh\left(\frac{\beta\hbar\omega}{2}\right) - \left(\frac{x-y}{2}\right)^2 \coth\left(\frac{\beta\hbar\omega}{2}\right)\right). \quad (30)$$

We note that at high temperature the first order coherence function for two particles is twice that of a single thermal particle [9]. This can be explained by the fact that the two-particle wave function is the product of two single-particle wavefunctions. The first order coherence function is shown in Figure 1. It is given by a Gaussian with a width proportional to $\coth(\beta\hbar\omega/2)$ in the direction $x + y$ and a width proportional to $\tanh(\beta\hbar\omega/2)$ in the direction $x - y$. This is associated with the fact that with increasing temperature the higher order modes are more likely to be occupied, so that the width of the wavepacket and therefore also the width of $G^{(1)}(x, x)$ increases. At the same time the correlation between the wavefunction at different positions and therefore also the width of $G^{(1)}(x, -x)$ decreases, as can be seen in Figures 1d, 1h and 1l.

In order to eliminate the influence of density fluctuations we can alternatively investigate the degree of first order coherence $g^{(1)}$ defined in (17). The modulus of this function is proportional to the visibility of interference fringes seen in experiments. At $T = 0$ we find by inserting (25, 26):

$$g^{(1)}_{\mathrm{B,D}}(x, y) = 1, \quad (31)$$

$$g^{(1)}_{\mathrm{F}}(x, y) = \frac{1 + 2xy}{\sqrt{(1 + 2x^2)(1 + 2y^2)}}, \quad (32)$$

as shown in Figures 2a–2d. The constant value of 1 indicates that bosons and distinguishable particles are first-order coherent at zero temperature, and in this way are reminiscent of classical stable waves or equivalently of a single mode. For fermions, however, the degree of first order coherence varies between coherent regions of $g^{(1)}_{\mathrm{F}}(x, y) = \pm 1$, and incoherence with $g^{(1)}_{\mathrm{F}}(x, -1/2x) = 0$. At these positions the amplitude of the first excited state destructively interferes with the amplitude of the ground state. At higher temperatures more modes contribute to the two-particle state so that the amplitude correlations diminish. Figures 2e–2l show how, with increasing temperature, the incoherent regions of all particles extend until at very high temperatures coherent behaviour can only be found for $g^{(1)}(x, x)$.

We now proceed to investigate the second order coherence function for particles at different temperatures. We begin by analysing the form of the second quantised formula for $G^{(2)}(x, y)$ (14, 16) at zero temperature. Again we are using the fact that two bosons or distinguishable particles are allowed to occupy the same ground state of the harmonic oscillator, whereas two fermions have to fill up the lowest two states, leading to

$$G^{(2)}_{\mathrm{B,D}}(x, y) = 2u_0^2(x)u_0^2(y) = \frac{2}{\pi} \exp\left(-(x^2 + y^2)\right), \quad (33)$$

$$G^{(2)}_{\mathrm{F}}(x, y) = (u_1(x)u_0(y) - u_0(x)u_1(y))^2 = \frac{2(x - y)^2}{\pi} \exp\left(-(x^2 + y^2)\right), \quad (34)$$

illustrated in Figures 3a–3d. The second order coherence function for bosons and distinguishable particles is given by a two-dimensional Gaussian centred around zero, whereas fermions show a bimodal distribution with peaks

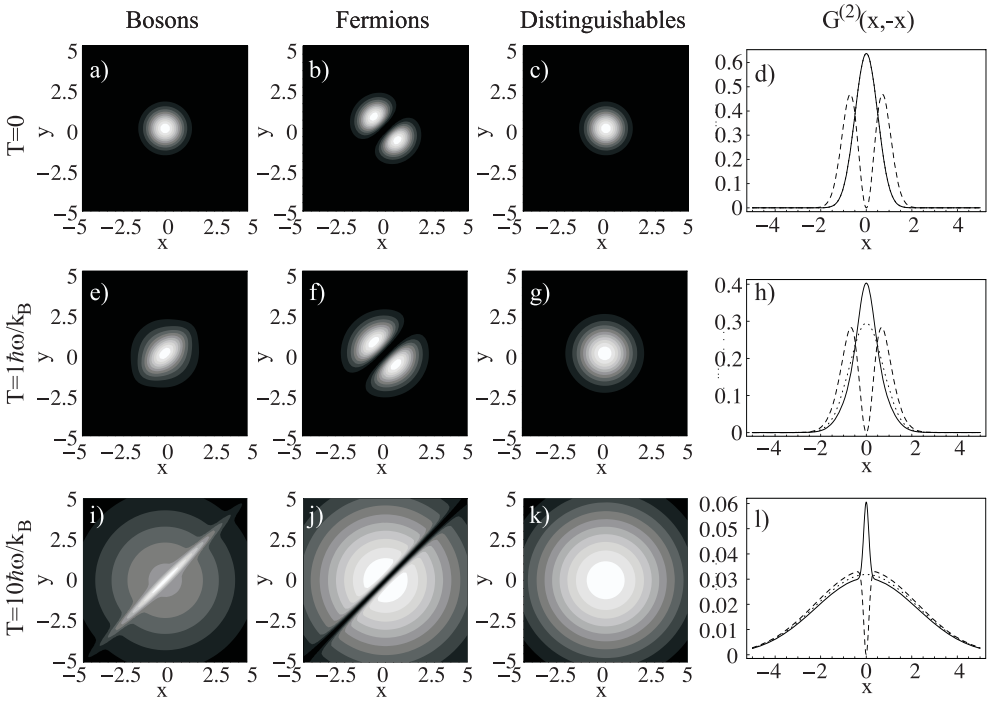

Fig. 3. Density plots of the second order coherence function $G^{(2)}(x,y)$ for two bosons, fermions and distinguishable particles at the temperatures $T = 0$, $T = \hbar\omega/k_{\mathrm{B}}$ and $T = 10\hbar\omega/k_{\mathrm{B}}$, displayed as in Figure 1.

at $x = -y = 1/\sqrt{2}$. As $G^{(2)}(x,y)$ is proportional to the probability of finding one particle at x and the other at y, $G^{(2)}_{\mathrm{F}}(x,x) = 0$ results directly from the exclusion principle for fermions. This result obviously holds for all temperatures.

For arbitrary temperatures, we evaluate $G^{(2)}(x,y)$ from equation (24):

$$G^{(2)}(x,y) = \frac{\kappa}{\sqrt{\pi}}\left(1+b^2\right)\exp\left(-\left(x^2+y^2\right)\tanh\left(\frac{\beta\hbar\omega}{2}\right)\right) + \frac{2b\kappa}{\sqrt{\pi}}\exp\left(-\frac{(x+y)^2}{2}\tanh\left(\frac{\beta\hbar\omega}{2}\right) - \frac{(x-y)^2}{2}\coth\left(\frac{\beta\hbar\omega}{2}\right)\right), \tag{35}$$

with κ given in (28). The behaviour of $G^{(2)}$ at various temperatures is shown in Figure 3. Unlike $G^{(1)}$, the second order coherence function always differentiates between bosons, fermions and distinguishable particles, even at high temperatures. For distinguishable particles, $G^{(2)}$ is given by a two-dimensional Gaussian with a width that increases with temperature as $2\coth(\beta\hbar\omega/2)$. For indistinguishable particles the Gaussian width in direction $x+y$ is $2\coth(\beta\hbar\omega/2)$ whereas the width in direction $x-y$ depends on the particle nature. Bose-enhancement leads to a preferred occupation of the same state and thus to a peak at $G^{(2)}_{\mathrm{B}}(x,x)$, whereas Fermi-exclusion leads to the vanishing of $G^{(2)}_{\mathrm{F}}(x,x)$. The plots of $G^{(2)}(x,-x)$ in Figures 3d, 3h and 3l illustrate how distinguishable particles with increasing temperature tend to behave like the average of fermions and bosons.

Again, we can eliminate the effect of density fluctuations by evaluating the degree of second order coherence according to (18). At zero temperature we find by inserting (25) and (34) for fermions or (26) and (33) for bosons or distinguishable particles:

$$g^{(2)}_{\mathrm{B,D}}(x,y) = \frac{1}{2}, \tag{36}$$

$$g^{(2)}_{\mathrm{F}}(x,y) = \frac{(x-y)^2}{2\left(x^2+\frac{1}{2}\right)\left(y^2+\frac{1}{2}\right)}, \tag{37}$$

illustrated in Figures 4a–4d. It is well-known from optics that anti-bunching of n particles in a single mode is associated with a value of $g^{(2)} = 1 - 1/n$ [3]. The constant value of $1/2$ for the degree of second order coherence thus indicates perfect anti-bunching of the two bosons or distinguishable particles at zero temperature. For distinguishable particles this is valid at any temperature and indeed for any state, however, it is a consequence of our definition of the coherence functions for distinguishable particles rather than a display of non-classical features. For fermions, $g^{(2)}$ at $T = 0$ varies between 0 and 1 at different positions. In particular, we find that $g^{(2)}_{\mathrm{F}}(x,x) = 0$ resulting from the Fermi-exclusion principle.

At arbitrary temperatures, the degree of second order coherence can be calculated analytically by inserting equations (27) and (35) into (18). For bosons and fermions the degree of second order coherence varies with temperature, as is illustrated in the first two columns of Figures 4 respectively. For bosons $g^{(2)}_{\mathrm{B}}(x,x)$ increases asymptotically from $1/2$ at zero temperature to 1 at high temperature, whereas for fermions $g^{(2)}_{\mathrm{F}}(x,x) = 0$ at all temperatures. The crucial dependence of the second order coherence on the particle nature can best be seen on

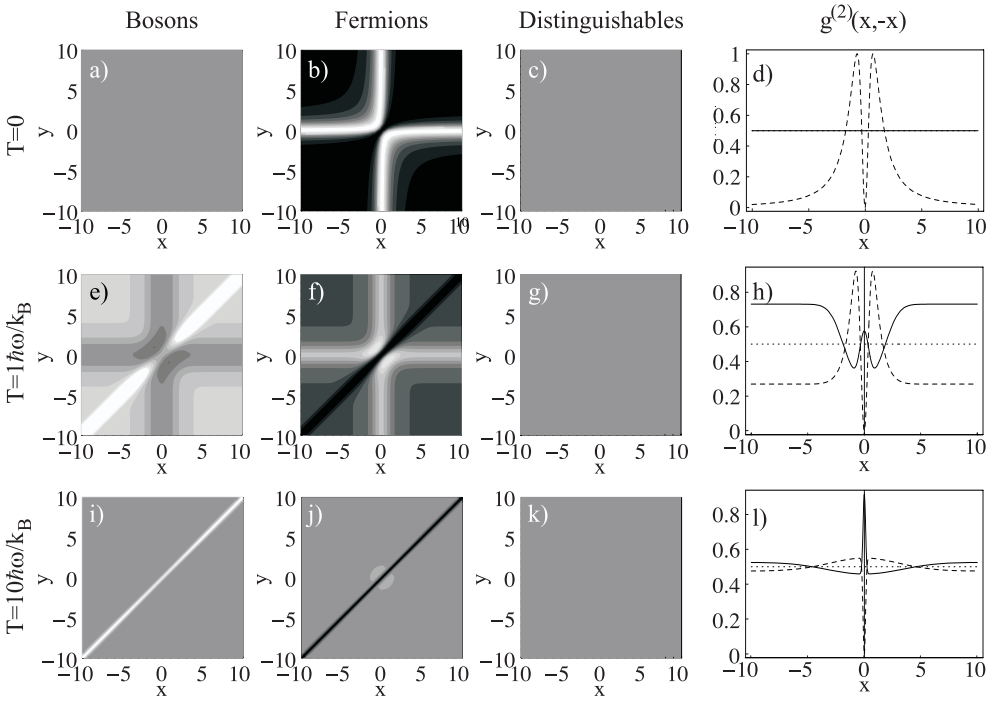

Fig. 4. Density plots of the degree of second order coherence $g^{(2)}(x,y)$ for two bosons, fermions and distinguishable particles at the temperatures $T = 0$, $T = \hbar\omega/k_{\rm B}$ and $T = 10\hbar\omega/k_{\rm B}$, displayed as in Figure 1.

$g^{(2)}(x,-x)$. This function is displayed in Figures 4d, 4h and 4l for different values of the temperature. At high temperature, $g^{(2)}_{\rm B}(0,0) \to 1$ for bosons, $g^{(2)}_{\rm F}(0,0) = 0$ and $g^{(2)}_{\rm D}(0,0) = 1/2$, whereas $g^{(2)}(x,-x) \to 1/2$ when $x \to \infty$ for all particles. Bosons clearly display bunching effects and fermions anti-bunching. This indicates that the degree of second order coherence is most suitable to display non-classical behaviour of the bosons and fermions, in analogy to its role in optics.

5 Coherence properties of interacting particles

Mathematically, interacting particles differ from non-interacting ones in that their relative motion is described by parabolic cylinder functions rather than by number states. By inserting the modes of relative motion (10) and the centre-of-mass modes (4) into (23) and (24) we find general expressions for the first and second order coherence functions, which can be numerically evaluated for any probability distribution $P_{n\nu}$. In this paper, however, we will concentrate on interacting particles at zero temperature as in this regime the interaction plays an important role. For higher temperatures the effect of interaction becomes less significant since the influence of the potential decreases for higher order modes as depicted in Figure 5. At $T = 0$ the centre-of-mass mode is given by $u_0(x_{\rm c}) = \pi^{-1/4}\exp(-x_{\rm c}^2)$ and the modes of the relative motion are given by the $w_\nu(x_{\rm r})$ from (10), where ν is the lowest value permitted by (12) for a given interaction strength a. A selection of these modes is shown by the solid lines in Figures 5b–5g. While for $a = 0$ the relative mode is given by a Gaussian, repulsive interaction will result in a sharper peak at $x_{\rm r} = 0$ and attractive interaction will decrease the mode function at $x_{\rm r} = 0$ until for an infinitely strong repulsion $v_\nu(0) = 0$. In fact, for $a \to \infty$ we know that $v_\nu(x_{\rm r}) = u_1(|x_{\rm r}|) = |u_1(x_{\rm r})|$.

The first and second order coherence function can then be evaluated from (23, 24):

$$G^{(1)}(x,y) = \frac{2}{\sqrt{\pi}}{\rm e}^{-(x^2+y^2)/2}\int_{-\infty}^{\infty}{\rm d}z\,{\rm e}^{-z^2-z(x+y)} \times w_\nu\left(\frac{z-y}{\sqrt{2}}\right)w_\nu\left(\frac{z-x}{\sqrt{2}}\right), \qquad (38)$$

$$G^{(2)}(x,y) = \frac{2}{\sqrt{\pi}}{\rm e}^{-(x+y)^2}w_\nu^2\left(\frac{x-y}{\sqrt{2}}\right)\cdot \qquad (39)$$

Since the width of the eigenmodes increases with increasing interaction, $G^{(1)}(x,x)$ becomes broader and develops a bimodal distribution for strongly repulsive interaction, as illustrated in Figure 6a. Similarly, also $G^{(1)}(x,-x)$ broadens with increasing interaction strength, shown in Figure 6b. At the same time, the shape of the first order coherence function changes from a narrow peak at $a \ll 0$, *via* a Gaussian at $a = 0$ to a wide peak "with shoulders" at $a \gg 0$. These appear at positions where the dent in the wavefunction of one particle overlaps with a peak of the other particle's wavefunction.

Due to the form of the interaction potential, the main influence on the second order coherence function occurs at the origin. According to (39), the function $G^{(2)}(x,x)$ is given by a Gaussian weighted with the squared parabolic cylinder function at the origin. This leads to a constant decrease of $G^{(2)}(x,x)$ with rising interaction strength, consistent with the fact that attracting bosons are more likely to be found at the same position whereas repelling bosons

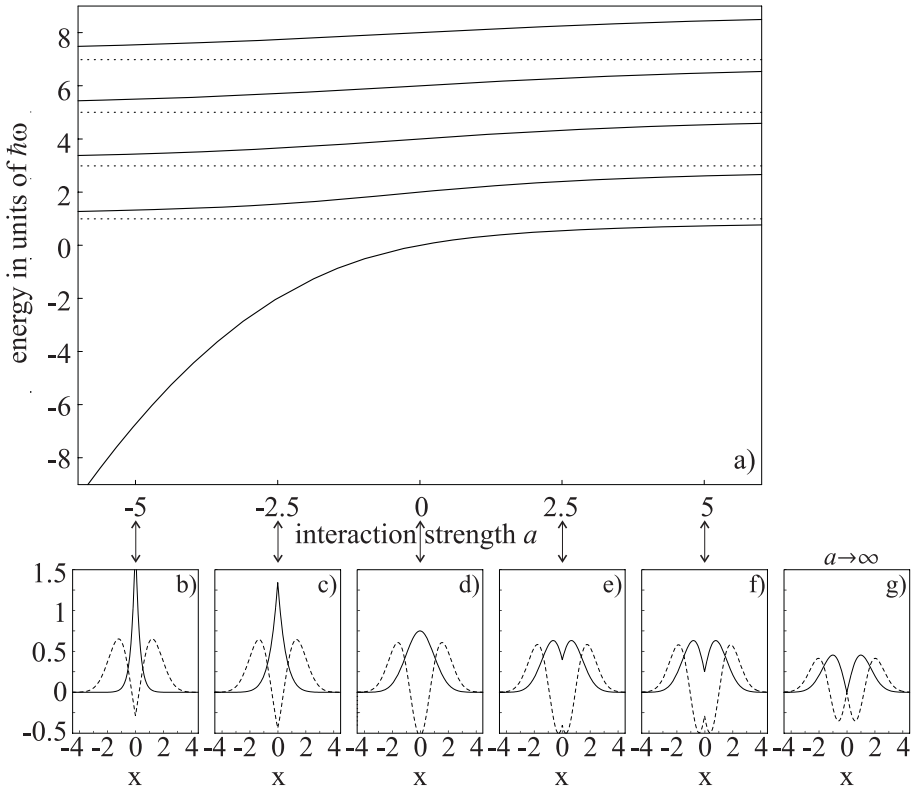

Fig. 5. (a) Energy levels of two interacting particles *vs.* the interaction strength a. Bosons fill up the levels shown as solid lines, whereas distinguishable particles can also occupy the levels shown as dotted lines. (b–g) Ground state (solid line) and first excited state (dashed line) wavefunctions of bosons for different interaction strengths $a = -5, -2.5, 0, 2.5, 5$ and $a \to \infty$.

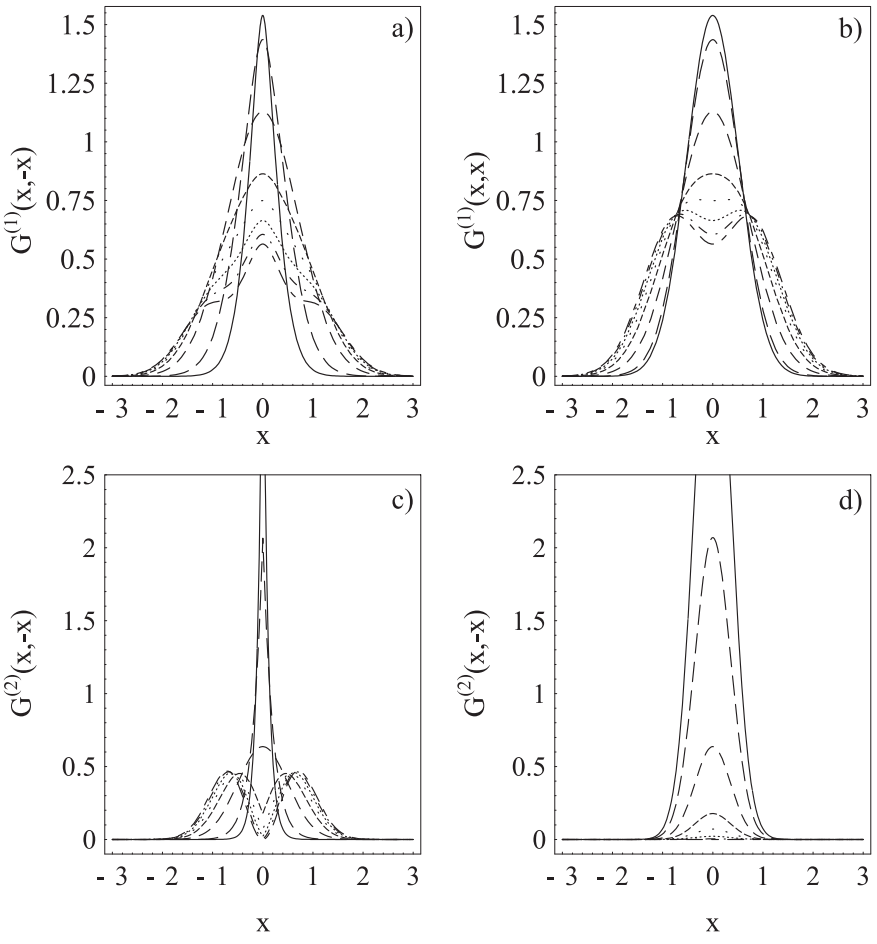

Fig. 6. First and second order coherence functions for bosons at zero temperature with various interaction strengths: (a) $G^{(1)}(x,x)$, (b) $G^{(1)}(x,-x)$, (c) $G^{(2)}(x,x)$ and (d) $G^{(2)}(x,-x)$. The different curves represent interaction strengths of $a = -5$ (solid lines), $a = -2.5$ (wide dashes), $a = 0$ (medium dashes), $a = 2.5$ (narrow dashes), $a = 5$ (wide dots), $a = 10$ (narrow dots), $a = 25$ (dot-dashes) and $a \to \infty$ (irregular dashes).

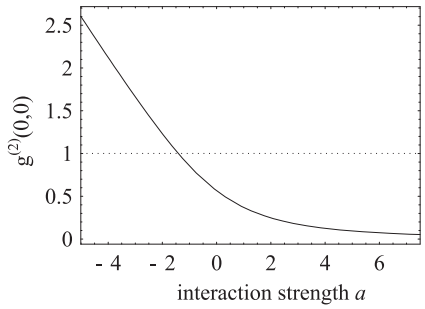

Fig. 7. Degree of second order coherence $g^{(2)}(0,0)$ for bosons at zero temperature as a function of the interaction strength a displaying bunching for a negative interaction strength and anti-bunching for a positive interaction strength. In this respect repelling bosons resemble fermions, whereas attracting bosons behave even more "boson-like".

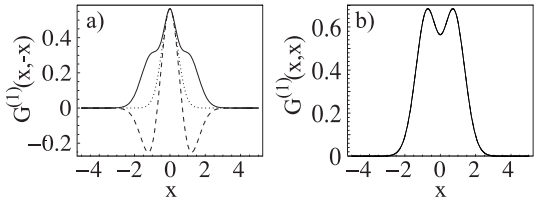

Fig. 8. (a) First order coherence function $G^{(1)}(x,-x)$ for infinitely strongly repelling bosons (solid lines), distinguishable particles (dotted lines) and non-interacting fermions (dashed lines) at zero temperature. (b) Along the direction $x = y$ the first order coherence function coincides for the three cases.

avoid this situation, as shown in Figure 6c. In the direction $x-y$, the second order coherence function is proportional to $w_\nu(\sqrt{2}x)$, leading to a sharp peak for attractive interaction and a bimodal distribution for repulsive interaction depicted in Figure 6d. The significance of this effect becomes clearer by studying the degree of second order coherence. Figure 7 shows the degree of second order coherence at the origin for varying interaction strength. We find that a negative interaction strength leads to bunching effects, while a positive interaction strength leads to anti-bunching. In this way repelling bosons resemble fermions, whereas attracting bosons behave even more "boson-like".

In the following we study the effects of an infinitely strong repulsive interaction in more detail. This case of particular interest as particles with $a \to \infty$ are forming a quantum Tonks gas, extensively studied in literature [12]. Their wavefunction is given by the modulus of the fermionic wavefunction allowing us to obtain analytic expressions for their coherence functions. We first note that the second order coherence function (24) contains only squared moduli of the mode functions. Consequently, $G^{(2)}(x,y)$ for Tonks particles and Fermions coincide. This result holds at all temperatures. The first order coherence function, however, depends on the amplitude of the wavefunction so that we expect differences for the behaviour of Tonks particles and fermions. For bosons with $a \to \infty$ at $T = 0$ we find

$$\begin{aligned} G^{(1)}(x,y) &= 2\int_{-\infty}^{\infty} \mathrm{d}z\, u_0\left(\frac{z+y}{2}\right) u_0\left(\frac{z+x}{2}\right) \\ &\quad \times \left|u_1\left(\frac{z-y}{2}\right)\right| \left|u_1\left(\frac{z-x}{2}\right)\right| \\ &= \frac{2}{\pi}\exp\left(-\frac{x^2+y^2}{2}\right)\int_{-\infty}^{\infty}\mathrm{d}z\,|z-y||z-x| \\ &= \frac{2}{\pi}\exp\left(-\frac{x^2+y^2}{2}\right) \\ &\quad \times \Big[-x\exp\left(-y^2\right) + y\exp\left(-x^2\right) \\ &\quad + \frac{\sqrt{\pi}}{2}(1+2xy)\left(1-\mathrm{erf}(y)+\mathrm{erf}(x)\right)\Big], \quad (40) \end{aligned}$$

where without loss of generality we have assumed that $x \le y$. We note that the first order coherence function along $x-y$ depends on the particle nature as shown in Figure 8a, whereas along $x+y$ it is identical for Tonks-Girardeau particles and fermions, see Figure 8b. The function $G^{(1)}(x,-x)$ contains negative regions for fermions, resulting from destructive interference between positive and negative regions of the fermionic wavefunction. The wavefunction of Tonks-Girardeau particles, however, are positive with a node at the origin. The corresponding first order coherence function is therefore entirely positive with turning points at the positions corresponding to an overlap of the node of one wavefunction with a peak of the other.

For completeness we also investigate the coherence properties of infinitely strongly repelling distinguishable particles at zero temperature. Distinguishable particles are allowed to occupy even and odd states of the relative motion. At $a \to \infty$ the energies of each pair of even and odd states coincides, so that distinguishable particles at $T \to 0$ may either be in the Tonks mode $|u_0(x_\mathrm{r})|$ or in the fermionic mode $u_0(x_\mathrm{r})$. If we take the limit of $T \to 0$ before $a \to \infty$, distinguishable particles will behave like Tonks-Girardeau particles, whereas if we take the limit $a \to \infty$ first they will behave like the average of Fermions and Tonks-Girardeau particles. This is the case shown by the dotted line in Figure 8. For distinguishable particles, $G^{(1)}(x,-x)$ shows neither negative regions like Fermions nor turning points like Tonks-Girardeau particles.

We note, finally, that the second order coherence function of two Tonks-Girardeau particles coincides with that of two fermions as only the squared modulus of the wavefunction enters the formula for $G^{(2)}(x,y)$ (24). This means that infinitely strongly repelling bosons show the same intensity interference as fermions.

6 Conclusion

We have demonstrated that many interesting features of statistical physics of bosons and fermions are already contained in the behaviour of two trapped particles. The first

order coherence function and the degree of first order coherence at zero temperature strongly depend on the particle nature, as in this case the Fermi-exclusion principle or the Bose-enhancement have a large impact on the respective wave functions. At higher temperatures these differences become less important and all particles show similar first order coherence. However, intensity fluctuations as measured by the second order coherence function depend crucially on the particle nature at all temperatures. At finite temperature, non-interacting bosons display bunching effects, while fermions show anti-bunching.

Furthermore, we have shown how a short range interaction between bosons and distinguishable particles alters the coherence properties. A strong repulsive interaction between bosons can lead to anti-bunching effects, whereas an attractive interaction increases the bunching effects. Bosons subject to an infinitely strong repulsive interaction model Tonks-Girardeau particles. Their second order coherence properties are identical to those of fermions, but their first order coherence properties differ.

Finally, we note that our analysis, based on one spatial dimension, can be extended to two or three spatial dimensions. In such a case, the potential of interaction has to be regularised [10,16,17] but we anticipate that the effects of particle nature and interaction obtained in this paper will survive the transfer to higher dimensions.

We thank Paul Radmore and Thomas Busch for their helpful comments. This work was supported by Enterprise Ireland under the International Collaboration programme and by the Leverhulme Trust. SFA and SMB thank the Royal Society of Edinburgh and the Scottish Executive Education and Lifelong Learning Department for the award of a Personal Research Fellowship and a Support Research Fellowship, respectively. GH thanks the Science Foundation Ireland for the award of the Investigator Programme research grant sfi/01/fi/co.

References

1. C.J. Pethick, H. Smith, *Bose-Einstein Condensation in Dilute Gases* (Cambridge University Press, Cambridge, 2002); Special issue on coherent matter waves, edited by K. Burnett, J. Phys. B **33**, 4177 (2000); `http://amo.phys.GaSoU.edu/bec.html`
2. M. Naraschewski, R.J. Glauber, Phys. Rev. A **59**, 4595 (1999)
3. R. Loudon, *The quantum theory of light* (Oxford University Press, Oxford, 1973)
4. L. Mandel, E. Wolf, *Optical coherence and quantum optics* (Cambridge University Press, Cambridge, 1995)
5. W. Ketterle, H.J. Miesner, Phys. Rev. A **57**, 3291 (1997)
6. E.A. Burt, R.W. Ghrist, C.J. Myatt, M.J. Holland, E.A. Cornell, C.E. Wieman, Phys. Rev. Lett. **79**, 337 (1997)
7. G. Huyet, S. Franke-Arnold, S.M. Barnett, Phys. Rev. A **63**, 043812 (2001)
8. S.M. Barnett, S. Franke-Arnold, A. Arnold, C. Baxter, J. Phys. B **33**, 4177 (2000)
9. S. Franke-Arnold, G. Huyet, S.M. Barnett, J. Phys. B **34**, 945 (2001)
10. The treatment in more than one dimension is non-trivial, see *e.g.*, Th. Busch, B.G. Englert, K. Rzazewski, M. Wilkens, Found. Phys. **28**, 549 (1998), and references therein
11. M.A. Cirone, K. Góral, K. Rzążewski, M. Wilkens, J. Phys. B **34**, 4571 (2001)
12. M.D. Girardeau, E.M. Wright, Laser Phys. **12**, 8 (2002); M.D. Girardeau, E.M. Wright, J.M. Triscari, Phys. Rev. A **63**, 033601 (2001); D.S. Petrov, G.V. Shlyapnikov, J.T.M. Walraven, Phys. Rev. Lett. **85**, 3745 (2000)
13. E. Andersson, M.T. Fontenelle, St. Stenholm, Phys. Rev. A **59**, 3841 (1999)
14. W. Ketterle, N.J. van Druten, Phys. Rev. A **54**, 656 (1996); A. Görlitz *et al.*, Phys. Rev. Lett. **87**, 130402 (2001)
15. *Handbook of mathematical functions*, edited by M. Abramowitz, I.A. Stegun (Dover Publications Inc., New York, 1964)
16. E. Fermi, Ricera Sci. **7**, 12 (1936)
17. E. Tiesinga, C.J. Williams, F.H. Mies, P.S. Julienne, Phys. Rev. A **61**, 063416 (2000)